Diagnostics of Carbon Nanotube Formation in a Laser Produced Plume:
An Investigation of the Metal Catalyst
by Laser Ablation Atomic Fluorescence Spectroscopy

Gary De Boer.
LeTourneau University
ES
August 4, 2000

Carl Scott
Thermal Branch
Structures and Mechanics Division
Engineering Directorate
NASA/JSC

Gary De Boer 8/3/00

Carl Scott 8/2/00

Diagnostics of Carbon Nanotube Formation in a Laser Produced Plume:
An Investigation of the Metal Catalyst
by Laser Ablation Atomic Fluorescence Spectroscopy

Final Report
NASA/ASEE Summer Faculty Fellowship Program – 1999
Johnson Space Center

Prepared By:	Gary D. De Boer, Ph.D.
Academic Rank:	Assistant Professor
University & Department	LeTourneau University Division of Natural Science
NASA/JSC	
Directorate:	Engineering
Division:	Structures and Dynamics Division
Branch:	Thermal
JSC Colleague	Carl Scott
Date Submitted	August 4, 2000
Contract Number	NAG-9-867

ABSTRACT

Carbon nanotubes, elongated molecular tubes with diameters of nanometers and lengths in microns, hold great promise for material science. Hopes for super strong light-weight material to be used in spacecraft design is the driving force behind nanotube work at JSC. The molecular nature of these materials requires the appropriate tools for investigation of their structure, properties, and formation. The mechanism of nanotube formation is of particular interest because it may hold keys to controlling the formation of different types of nanotubes and allow them to be produced in much greater quantities at less cost than is currently available.

This summer's work involved the interpretation of data taken last summer and analyzed over the academic year. The work involved diagnostic studies of carbon nanotube formation processes occurring in a laser-produced plume. Laser ablation of metal doped graphite to produce a plasma plume in which carbon nanotubes self assemble is one method of making carbon nanotube. The laser ablation method is amenable to applying the techniques of laser spectroscopy, a powerful tool for probing the energies and dynamics of atomic and molecular species.

The experimental work performed last summer involved probing one of the metal catalysts, nickel, by laser induced fluorescence. The nickel atom was studied as a function of oven temperature, probe laser wavelength, time after ablation, and position in the laser produced plume. This data along with previously obtained data on carbon was analyzed over the academic year. Interpretations of the data were developed this summer along with discussions of future work.

The temperature of the oven in which the target is ablated greatly influences the amount of material ablated and the propagation of the plume. The ablation conditions and the time scale of atomic and molecular lifetimes suggest that initial ablation of the metal doped carbon target results in atomic and small molecular species. The metal atoms survive for several milliseconds while the gaseous carbon atoms and small molecules nucleate more rapidly. Additional experiments and the development of *in situ* methods for carbon nanotube detection would allow these results to be interpreted from the perspective of carbon nanotube formation.

INTRODUCTION

Nanotechnology, the use of materials with dimensions of nanometers, represents engineering at the molecular scale. Many of the promises of nanotechnology have focussed on the use of nanometer scaled tubes discovered in 1991. [1] These tubes with dimension of nanometers in diameter and microns in length can be described as elongated fullerenes, and are often referred to as "nanotubes." Though nanotubes can be composed of combinations of carbon, nitrogen, and boron, [2] it is the pure carbon nanotube that has dominated discussions and has been the focus of the research at NASA/JSC. The molecular structure of the carbon nanotube is the source of its unique properties and technological promise. [3-16] The physical properties associated with a network of chemical bonds and aspect ratios of several orders of magnitude imply that incredibly strong, lightweight composite materials can be formed using nanotubes. [4-6] Another application of nanotubes may include hydrogen storage with potential benefits to fuel cell development. [7, 8] Nanotubes have conductivity ranging from that of insulator to metallic conductor as a function of their geometry and size [9-13] leading to exciting implications for electronic applications. Because of the promising potential of carbon nontubes, NASA has made a commitment to take an active part in this cutting edge research and is currently producing, purifying, characterizing, and performing composite studies with carbon nanotubes.

Though promising methods have been developed recently for the large-scale production of nanotubes, the reality of gross quantities of inexpensive materials has remained elusive. Therefore, to advance NASA's objective of developing nanotube materials for space applications, processes that provide reproducible, inexpensive, bulk materials with specific properties are needed.

The objective of this work has been to obtain a better understanding of carbon nanotube formation for purposes of increasing production and enabling further research into composites and other materials. The self-assembly of carbon nanotubes involving species at the atomic and molecular level requires the use of appropriate tools. The most powerful tools of chemists and molecular physicists are those of atomic and molecular spectroscopy. Carbon nanotube production by laser ablation provides an environment for the spectroscopic probing of carbonaceous materials and metal atoms. Specific spectroscopic techniques employed include resolved emission and laser induced fluorescence. Atomic fluorescence spectroscopy is an extremely sensitive means of detecting a variety of metals [17-22] including nickel. [23-25] In this work atomic fluorescence spectroscopy has been employed to probe the metal catalyst during the production of carbon nanotubes by laser ablation. The metal signal was measured as a function of the same parameters used in previous carbonaceous studies at JSC allowing the carbonaceous and metal data to be complementary.

EXPERIMENTAL

The nanotube production setup at JSC follows that developed at Rice University [26] described previously by Arepalli, *et al.* [27, 28] Briefly, the setup includes a carbon target (19 mm diameter) which is doped with 1% nickel and 1% cobalt and is supported on a rod in an oven which is heated to 1473 K during normal production. The target and rod are centered within a 50.8 mm quartz tube. A smaller 25.4 mm quartz tube is centered within the 50.8 mm tube and extends to 6 mm of the target. Argon flows through the tubes toward the target at a pressure of 67 kPa and a flow rate of 100 sccm. Two Nd:YAG ablation lasers follow a path through the inner tube to strike the flat end of the target at normal incidence. The green (532 nm) Nd:YAG laser fires 50 ns prior to the IR (1064 nm) Nd:YAG laser. The ablations lasers, which generally operate at 60 Hertz, were operated at 10 Hertz for these experiments with an average power output of 1.5 watts and an energy density of 1.6 J/cm^2 per pulse for a laser spot size diameter of 3.4 mm. A third Nd:YAG laser (355 nm) operating at 10 Hz is used to pump a Lambda Physik FL 3002 dye laser. The dye (Coumarin 120) laser output was frequency doubled with a BBO1 crystal and was tuned to the atomic lines of nickel over the wavelength range of 224.2 nm to 226.2 nm.

Two SRS digital delay generators and a 60-hertz to 10-hertz converter synchronized the lasers. Fluorescence from nickel metal atoms was focussed by a 200 mm focal length lens onto a 1 mm pinhole in front of a Hamamatsu R928 photomultiplier tube (PMT). Fluorescence spectra were acquired by monitoring the PMT signal as a function of dye laser wavelength, laser energies, PMT position, and pump-probe delay. The signals were averaged through a boxcar and the averaged signals were recorded with a PC. The time decay of nickel fluorescence was monitored with a LeCroy transient digitizer and a Tektronix digital oscilloscope. Emission was also collected with an optical fiber and a Spex 270M spectrophotometer that was used to resolve the emission. The resolved emission was recorded with an ICCD.

Wavelengths shorter than 350 nm for excitation and emission of the nickel atom were chosen to avoid spectral interference due to black body radiation produced by the oven and the carbonaceous emissions resulting from ablation. Also, the PMT is more sensitive in this range. The nature of the production setup results in a great deal of scattered incident radiation from the ablation and probe lasers. To reduce the detection of scattered probe radiation a combination of excitation and fluorescent lines was chosen to allow detection of only the fluorescing radiation. The excitation wavelength was varied from 224.2 and 226.2 nm while collecting fluorescence transitions between 290-310 nm. A Solar Blind (SB300) filter centered at 300 nm was placed in front of the PMT, allowing detection of the 300 nm fluorescence, while minimizing the detection of scattered ablation light, scattered dye laser light, and black body radiation. A diagram of the diagnostic setup and physical principles appear in Figures 1 and 2.

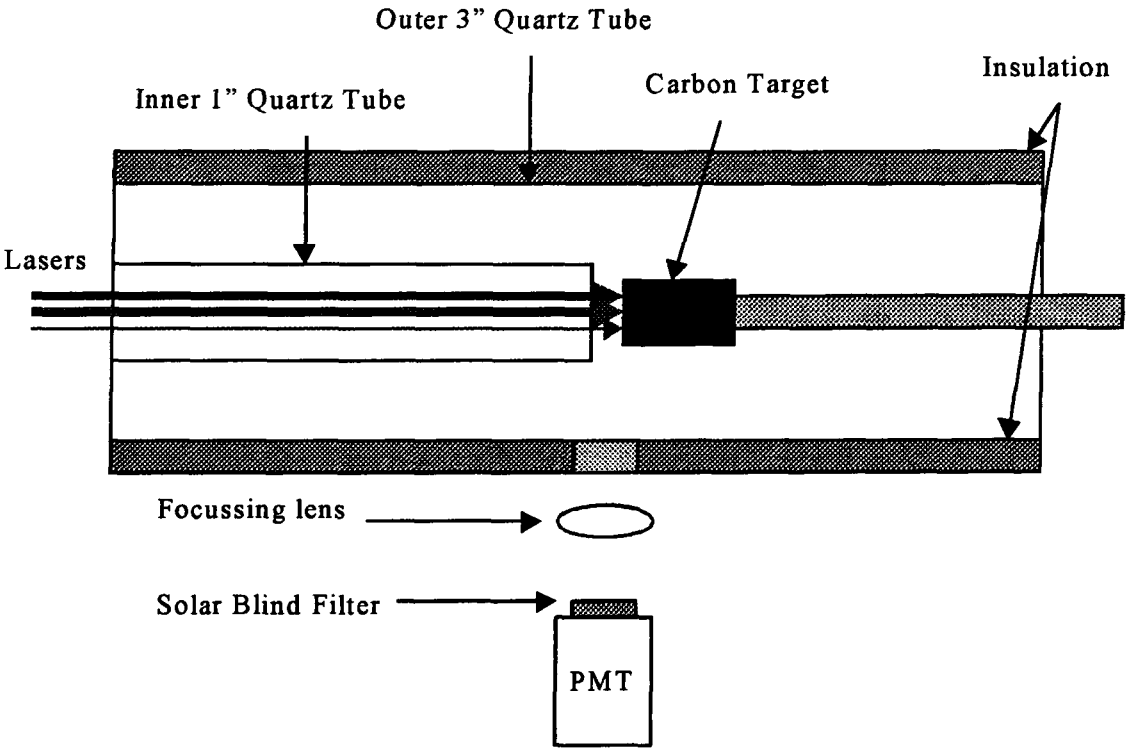

Figure 1. Diagnostics Setup

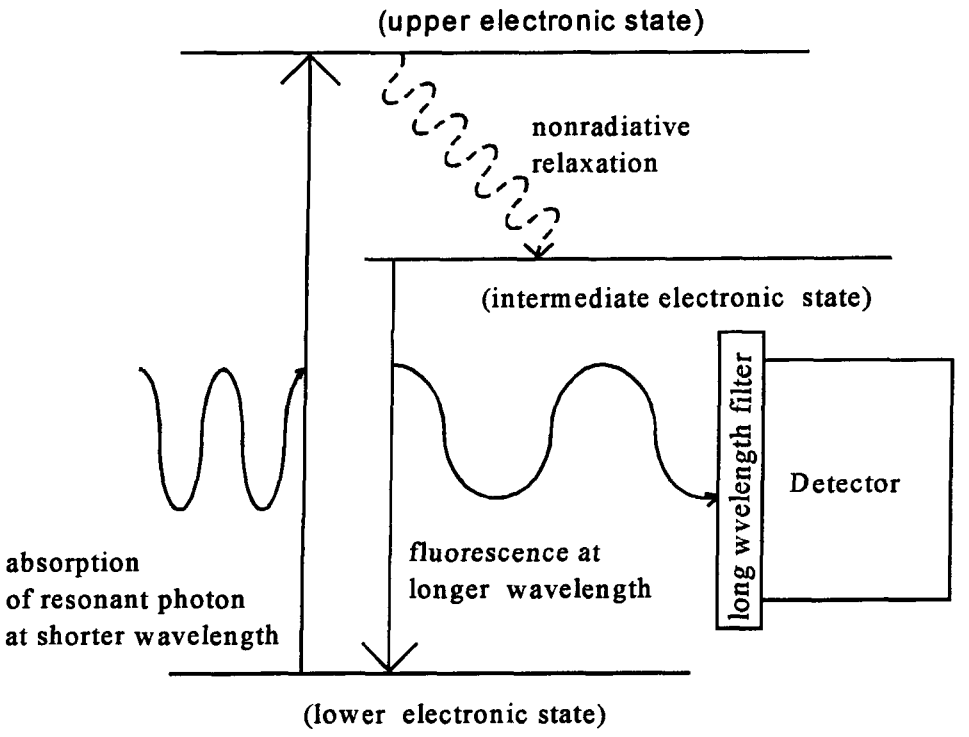

Figure 2. Illustration of Physical Principles

RESULTS

The nickel signal was recorded as a function of the pump-probe delay while positioning the PMT to collect the plume image 1 mm from the target surface, Figure 3. The nickel signal is seen even when probing within nanoseconds of the second ablation laser, though interference from the ablation lasers make quantifying the nickel fluorescence difficult. For the room temperature solid nickel target, Figure 3 inset, the nickel signal soon diminishes within a few microseconds, then increases only to diminish again within 20 μs of ablation. At an oven temperature of 1473 K the pump-probe time profile for the composite target appears to be quite different as it results in a long-lived signal of over several milliseconds, Figure 3. It can also be seen that the temporal peak of the nickel signal comes later in time as we probe farther from the target's surface. Imaging the plume at a distance of 1 mm, 2 mm, and 3 mm from the surface results in a change in the temporal profile implying a propagation velocity of about 10 m/s.

Wavelength spectra were taken over 224.2 nm to 226.2 nm. The transitions within this region involve electronic transitions from 3d to 4p atomic orbitals. Given that our line intensities are proportional to the intensity of the excitation transition, the line intensity can be related to the population of the lower states if the transition probabilities and degeneracies of the lower states are known. A distribution of the population of the lower states can be fit to a Maxwell-Boltzmann distribution to determine an electronic excitation temperature. The result of such an analysis at two different pump-probe delays for the composite target at 1473 K, along with a comparison to synthetic spectra of indicated temperature appears in Figure 4. The upper spectrum, A, in Figure 4 was taken at a pump probe delay which corresponds to the peak of the nickel signal intensity. The experimental data, circles, is compared to a synthetic spectrum generated with an electronic temperature of 1500 K. The lower spectrum, B, in Figure 4 was taken at a much earlier pump-probe delay which corresponds to much lower nickel signal intensity. The experimental data in B is compared with a synthetic spectrum generated with an electronic temperature of 225 K. Warmer electronic temperatures are associated with greater nickel atom signal intensities. This is true of both the solid nickel target at room temperature and the composite target heated to 1473 K by use of the oven.

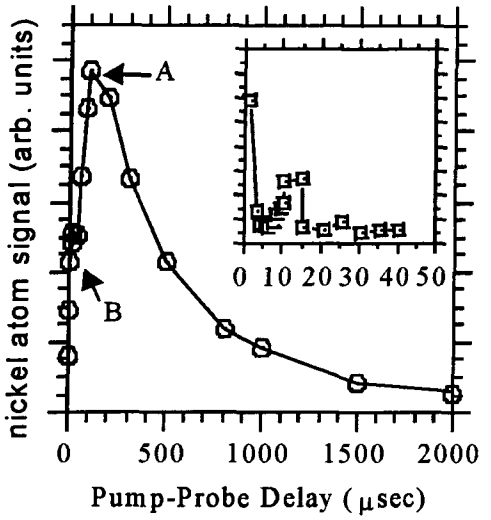

Figure 3

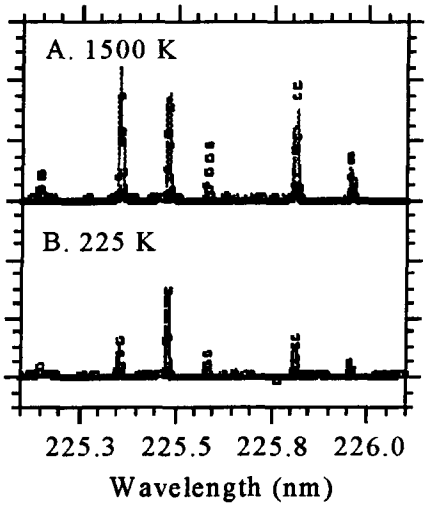

Figure 4

A similar analysis of previously obtained C_2 LIF spectra was also done. The analysis indicates a shorter lifetime for the C_2 species and cooler temperatures than for the nickel atom. The cooler temperatures are likely the result of only one laser being used for ablation, while two lasers were used in the nickel work. But as with the nickel data, the higher signal intensities relate to warmer temperatures, see Figures 5 and 6. The data in Figure 5 were collected at a pump-probe delay of 1 μs while the data in Figure 6 were collected with a fixed imaging distance of 1.75 mm.

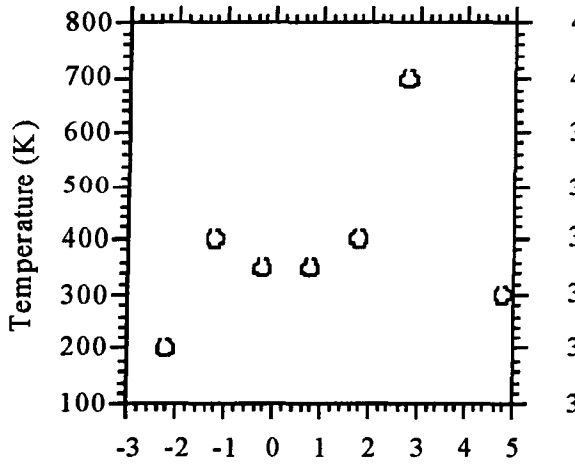

Figure 5

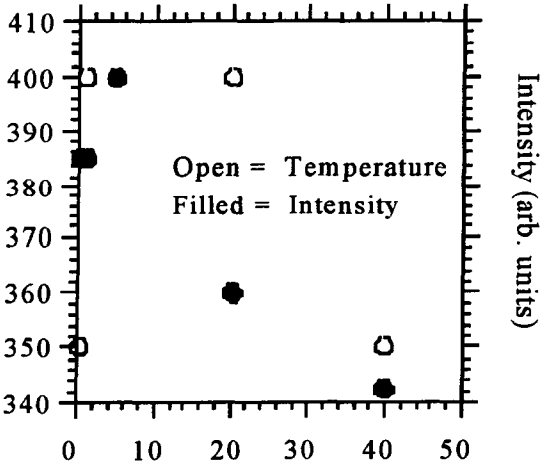

Figure 6

The LIF of both the C_2 and the nickel atom both are much lower by some thousands of Kelvin than the temperature indicated by C_2 emission. C_2 emission is more closely related to the plasma temperature.

DISCUSSION AND INTERPRETATION

Since metal catalysts are essential to carbon nanotube formation, several studies have focussed on the behavior of the metal. Yudasaka *et al* [29] have shown, by inspection of targets, that when Nd:YAG pulsed lasers are used there is poor metal ablation at room temperature and carbon nanotubes do not form. However, when the target is heated to 1473 K carbon nanotubes form and the metal is ablated from the target. Yudasaka also notes that when a CO_2 laser is used at room temperature carbon nanotubes are also formed, implying that the elevated ambient gas temperature is not necessary for nanotube assembly, but rather for metal ablation. [30] The microsecond CO_2 laser has a much longer pulse than the nanosecond Nd:Yag or excimer lasers. It is possible that the longer heating time of the CO_2 laser allows for better ablation so that elevated oven temperatures are not necessary. This work is consistent with an increase in nickel metal ablation at elevated oven temperatures. This work also indicates that the electronic temperature of nickel atoms produced by laser ablation is at least 1500 K in the center of the plume regardless of oven temperature and becomes much lower outside of the plume. The propagation and the lifetime of nickel atoms clearly change when the oven is used to elevate the target temperature.

Temperatures obtained from the nickel and carbon LIF spectra are much cooler than those indicated by the C_2 emission. Similar LIF and emission studies done by Brinkman [31] in a DC arcjet for purposes of analyzing diamond deposition found similar temperature differences between C_2 emission and LIF. Temperature measurements based on a variety of methods in other systems appear to give similar temperature variations for the electronically excited state and ground state species. [32-34] Brinkman postulates that the quenching of the excited electronic C_2 species is much faster than a multiple collision process necessary for reaching vibrational and rotational thermal equilibrium. The hot C_2 emission has a lifetime of about 60 μs implying that during this time short-lived C_2 species are being formed.

Laser produced plumes associated with carbon have been studied. [35-37] These studies indicate that the carbonaceous emission results primarily from recombination of atomic carbon to produce hot C_2 emission spectra. Arepalli *et al.* [38] have also explored the possibility that C_2 emission can result from the photodissociation or "shrinkage" of fullerenes. Both of these sources and possibly others are likely contributors to the hot C_2 emissions.

Computational studies based on analysis of the endcaps of carbon nanotubes formed in the DC arc indicate that the growth of carbon nanotubes occurs at between 700-1800 K, rather than the much higher temperatures of the plasma. [39] The dependence of nanotube diameter on oven temperature would also indicate that oven temperatures have a role in the formation process. [40] Arepalli et al. [28] have shown that oven temperature influences plume propagation, size and lifetime when Nd:YAG lasers are used for ablation. They

have also shown that target position relative to the inner tube can affect the plume propagation. The empirically determined optimal target position for the formation of carbon nanotubes also relates to the position in which the plume appears to have the slowest rate of propagation. No doubt the distance of the target from the inner tube influences the argon gas flow characteristics around the target. Yudasaka et al. [41] also notes that nickel ablation has a gas pressure dependency, though they attribute this dependency to effects on ablation rather than plume propagation. The ablation process very much influences the propagation of the plume and so it is difficult analyze them independently.

In regards to the metal species within the plume, whether they are atomic or large micrometer sized particle or melts, works to characterize plumes produced by laser ablation can be elucidative. [35-37, 42-46] Plumes associated metals, including nickel, have also been studied. [43-46] In general, it has been found that higher laser energy densities and gas pressures appear to be necessary to create metallic nanoparticles or liquid droplets by laser ablation. [43-45] Given the conditions of our experiments it seems likely that initial ablation results in atomic and small molecular species with the larger particles and droplets being less prevalent.

Dillon *et al* [47] have addressed the specific question of carbon nanotube formation as a function of laser parameters. They studied the formation of carbon nanotubes using pulsed lasers at 3 to 24 kHz with various pulse energies and continuous wave lasers indicate that tubes are formed at higher laser powers, but with lower pulse energies and higher pulse frequency, consistent with smaller species being ablated. This implies that the formation of carbon nanotubes is favored by species that are in the vapor phase.

Lifetimes of the C_2 and nickel atoms reported in this work indicate that nickel atoms are more prevalent than nickel particles or droplets. The long lifetime of the nickel atom signal would suggest that the presence of the atomic species is more prevalent than nickel particles or droplets. Lifetimes of emission and LIF of C_2 are shorter than the lifetime of the nickel LIF signal which may indicate that the nucleation process for carbon is faster than for the nickel metal. Geohegan observed a similarly long lifetime for the cobalt atom,[48] consistent with the suggestion that more metal atoms rather than metal clusters or particles are present during the first several milliseconds after ablation.

Maiti reports experimental nanotube growth rates of 1-500 A/ms for the DC arc process and calculates a growth rate of 8.2E2 A/ms at 1500 K and 1.9E4 A/ms at 2000 K based on molecular dynamics simulations. [49] This would imply a growth time of one to many milliseconds for a micron long tube. Smalley [50] and Scott *et al.* [51] propose much shorter microsecond times for nanotube formation during laser ablation, while Puretz *et al* [52] propose formation times of as long as seconds. Time scales on the order of milliseconds and longer would allow for metal nucleation during nanotube formation. The nucleation of metals into small bimetallic clusters may be the reason for a bimetallic dependence of

the metal catalyst. Clearly, additional efforts to determine the growth rates of nanotubes and the presence of nanotubes during the formation process are necessary.

This work demonstrates that nickel metal catalyst can be monitored *in situ* during carbon nanotube formation. Elevation of the oven temperature increases the amount of ablation and also appears to influence plume expansion and propagation. The distribution of energies in the nickel atom and the rotational energies of the ground electronic state of the C_2 species inferred from the LIF spectra, imply that the temperatures of these species are much lower than the plasma temperature. The temperatures determined by LIF are more closely related to the ambient oven temperature. Laser power densities, gas pressures, as well as metal and C_2 lifetimes are consistent with an atomic or small molecule presence upon ablation. Nucleation of bimetallic clusters during the time frame of nanotube growth is possible. The inner tube and gas properties may play an important role in the confining of reactive species during the formation process. Additional experiments including LIF studies of C_2 using two ablation lasers, additional LIF studies of nickel and cobalt as a function of various system parameters, and an *in situ* method to monitor nanotube growth would be beneficial to this work.

REFERENCES

1 Iijima, *Nature* **354**, 56 (1991).

2 S. IIjima, H. G. Zhang, and K. Suenaga, *Chemical Physics Letters* **279**, 264 (1997).

3 P. Calvert, in *Carbon Nanotubes Preparation and Properties*, edited by T. W. Ebbesen (NEC Research Institute, Princeton, New Jersey, 1996).

4 P. Calvert, *Nature* **399**, 210 (1999).

5 H. D. Wagner and O. Lourie, *Applied Physics Letters* **73**, 3527 (1998).

6 C. Bower, R. Roson, L. Jin, J. Han, and O. Zhou, *American Institute of Physics* **74**, 3317 (1999).

7 N. M. Rodriguez, A. Chambers, C. Park, and T. K. Baker, *The Journal of Physical Chemistry B* **102**, 4253 (1998).

8 A. C. Dillon, K. M. Jones, T. A. Bekkedah, C. H. Klang, D. S. Bethune, and M. J. Heben, *Nature* **386**, 377 (1997).

9 R. Smalley, J. W. G. Wildoer, L. C. Venema, A. G. Rinzler, and C. Dekker, *Nature* **391**, 59 (1998).

10 M. Burghard, A. Y. Kasumov, R. Deblock, M. Kociak, B. Reulet, H. Bouchiat, I. I. Khodos, Y. B. Gorbatov, V. T. Volkov, and C. Journet, *Science* **284**, 1508 (1999).

11 N. Hamada, *Material Science and Engineering* **B19**, 181 (1993).

12 J.-C. Charlier, *J. Mater. Res.* **13**, 2368 (1998).

13 J.-C. Charlier and P. Lambin, *The American Physical Society* **57**, 57 (1998).

14 C. Dekker, *Physics Today*, 22 (1999).

15 T. W. Ebbesen, *Carbon Nanotubes Preparation and Properties* (NEC Research Institute, Princeton, New Jersey, 1996).

16 J. Sloan, J. Cook, and M. Green, *Chemisty and Industry* **16**, 600 (1996).

17 W. Sdorra and K. Niemax, *Inst. Phys. Conf. Ser.* **11**, 463 (1990).

18 Y. Oky, T. Tani, N. Kidera, and M. Maeda, *Optics Communications* **110**, 298 (1994).

19 J. D. Winefordner, S. J. Weeks, and H. Haraguchi, *Analytical Chemistry* **50**, 360 (1978).

20 R. G. Michel, J. X. Zhou, X. Hou, and S.-J. J. Tsai, *Analytical Chemistry* **69**, 490 (1997).

21 R. g. Michel, J. P. Dougherty, and F. R. Preli, *Journal of Analytical Atomic Spectrometry* **2**, 429 (1987).

22 M. Maeda, Y. Oki, and E. Tashiro, *Analytical Chemistry* **65**, 2096 (1993).

23 J. D. Winfordner, M. S. Epstein, J. Bradshaw, S. Bayer, J. Bower, and E. Voigtman, *Applied Spectroscopy* **34**, 372 (1980).

24 O. Axner, A. Marunkov, N. Cherkalin, and J. Enger, *Spectrochimica Acta* **49B**, pp. 1385 (1994).

25 O. Axner, A. Marunkov, N. Chekalin, and J. Enger, *Spectrochimica Acta* **49B**, 1385 (1994).

26 R. E. Smalley, A. Thess, R. Lee, P. Nikolaev, D. Hongjie, P. Petit, J. Robert, C. Xu, Y. H. Lee, S. G. Kim, A. G. Rinzler, D. T. Colbert, G. E. Scuseria, D. Tomanek, and J. E. Fischer, *Science* **273**, 483 (1996).

27 S. Arepalli and C. D. Scott, *Chemical Physics Letters* **302**, 139 (1998).

28 S. Arepalli, P. Nikolaev, W. Holmes, and C. D. Scott, *Applied Physics A* **70**, 125 (2000).

29 M. Yudasaka, R. Kikuchi, O. Yoshimasa, O. Etsuro, and S. Yoshimura, *Appl. Phys. Lett.* **70**, 1817 (1997).

30 M. Yudasaka, S. Iijima, F. Kokal, K. Takahashi, R. Yamada, N. Sensui, and T. Ichihashi , *Journal of Physical Chemistry* **103**, 3576 (1999).

31 E. A. Brinkman, G. A. Ralche, M. S. Brown, and J. B. Jeffries, *Appl. Phys. B* **64**, 689 (1996).

32 J. A. Pobst, I. J. Wysong, and R. A. Spores, *IEPC* **95**, 203 (1995).

33 G. A. Raiche and J. B. Jeffries, *Appl. Opt.* **32**, 4629 (1993).

34 A. G. Gaydon, *The Spectroscopy of Flames, 2nd ed.* (Haisted, New York, 1974).

35 c. Parigger, D. H. Plemmons, J. O. Hornkohl, and J. W. L. Lewis, *J. Quant. Spetrosc. Radiat. Transfer* **52**, 707 (1994).

36 S.-i. Aoqui, t. Ikegami, Y. Yamagaa, and K. Ebihara, *Thin Solid Films* **316**, 40 (1998).

37 J. Seth, R. Padiyath, and S. V. Babu, *Appl. Phys. Lett.* **63**, 126 (1993).

38 S. Arepalli, C. D. Scott, P. Nikolaev, and R. E. Smalley, *Chemical Physics Letters* **320**, 26 (2000).

39 V. H. Crespi, *Physical Review Letters* **82**, 2908 (1998).

40 S. Bandow, S. Asaka, Y. Saito, A. M. Rao, L. Grigorian, E. Richter, and P. C. Eklund, *Phys. Rev. Lett.* **80**, 3779 (1998).

41 M. Yudasaka, T. Komatsu, Y. Ichihashi, Y. Achiba, and S. Iijima, *J. Phys. Chem. B* **102**, 4892 (1998).

42 C. Miller, *Laser Ablation Principles and Applications* (Springer, Berlin, 1994).

43 M. F. Becker, J. R. Brock, H. Cai, D. E. Henneke, J. W. Keto, J. Lee, W. T. Nichols, and H. D. Glicksman, *NanoStrucured Materials* **10**, 853 (1998).

44 K. H. Song and X. Xu, *Applied Surface Science* **127-129**, 111 (1998).

45 J. A. Aguilera, C. Aragon, and F. Penalba, *Applied Surface Science* **127-129**, 309 (1998).

46 M. Tanaka, Y. Fujisawa, T. Nakajima, Y. Tasaka, and K. Ota, *J. Appl. Phys.* **83**, 3379 (1998).

47 A. C. Dillon, P. A. Parilla, K. M. Jones, g. Riker, and M. J. Heben, *Advances in Laser Ablation of Materials (USA)*, 403 (1998).

48 A. A. Puretzky, D. B. Geohegan, X. Fan, and S. J. Pennycook, *Appl. Phys. Letts.* **76**, 182 (2000).

49 A. Maiti, C. J. Brabec, C. Ronald, and J. Bernholc, *Phys. Rev., Condens. Matter.* **52**, 14850 (1995).
50 R. E. Smalley, *Accounts of Chemical Research* **25**, 98 (1992).
51 C. D. Scott, S. Arepalli, P. Nikalaev, and R. Smalley, *to be published*, (2000).
52 A. A. Puretzky, D. B. Geohegan, X. Fan, and S. J. Pennycook, *Appl. Phys. A* **70**, 153 (2000).